16/12/2018

Correlazione Elettroencefalografica a distanza: ri-analisi di due studi tramite “machine-learning”

Marco Bilucaglia*, Luciano Pederzoli^, William Giroldini^, Elena Prati^, Patrizio Tressoldi°

*Behavior and BrainLab, IULM Università di Milano, Italy
^EvanLab, Firenze, Italy
°Science of Consciousness Research Group, Dipartimento di Psicologia Generale, Università di Padova, Italy

Corresponding author:
Patrizio Tressoldi
Email: patrizio.tressoldi@unipd.it

Riassunto

In questo studio sono stati ri-analizzati, tramite algoritmi di machine-learning, i dati ricavati da due studi relativi alla relazione tra le attività elettroencefalografiche (EEG) di una coppia di soggetti isolati e fisicamente separati.

Il primo insieme di dati era stato ricavato da 25 coppie di partecipanti e la stimolazione applicata ad uno dei due membri di ciascuna coppia era composta da segnali continui, visivi ed uditivi a 500 Hz, applicati simultaneamente per 1 secondo.

L'altro insieme di dati era stato ricavato da 20 coppie di partecipanti e un membro di ciascuna coppia aveva ricevuto, per 1 secondo, stimoli, visivi e uditivi a 900 Hz, modulati ON-OFF a 10, 12 e 14 Hz.

Una volta applicato un algoritmo del tipo 'linear discriminant classifier', nel primo insieme di dati è stato possibile classificare correttamente il 50,74% dell'attività elettroencefalografica dei partecipanti non stimolati come correlata alla stimolazione sensoriale remota.

Nel secondo insieme di dati la percentuale dell'attività elettroencefalografica dei partecipanti non stimolati correttamente classificata è stata 51,17%, 50,45% e 51,91% rispettivamente per le stimolazioni a 10, 12 e 14 Hz.

L'analisi dell'attività elettroencefalografica tramite algoritmi di machine-learning ha generato progressi nello studio della connessione tra le attività EEG del partner stimolato e quelle del partner isolato a distanza, evidenziando che tale relazione esiste anche in riferimento alla frequenza di stimolazione. Questo fenomeno aprirà nuove possibilità d'indagine della connessione non convenzionale tra i segnali EEG di soggetti fisicamente separati.

NOTA: L'articolo è scritto in linguaggio specialistico, quindi è riservato solo a coloro che, conoscendo a fondo gli argomenti trattati, non hanno difficoltà a leggere il testo direttamente in inglese.

Keywords: EEG, correlation at distance, machine learning, linear discrimination analysis.

Introduction

The test of whether or not the brain activities of two people who are only linked mentally – and with absolutely no other form of conventional communication – are correlated is a small research field that has existed for about 50 years (see Table S1 in Giroldini et al., 2016).
Despite accumulating evidence in favour of this correlation, this phenomenon is still considered controversial because, of the proposed theories to explain it, no single theory is widely accepted.
This correlation excludes the possibility of it originating from information received via the sense organs or from any direct link, even internet connections [see for example (Jiang et al., 2018; Lee et al., 2017)], or from the EEG activity of each member of participant pairs, given their physical distance and isolation from each other.
We are left with postulating a type of quantum-like connection based on the distant mental connection between each partner (Walach & Römer, 2011; Walach, Tressoldi, & Pederzoli, 2016; Galli Carminati, Martin, & Carminati, 2017), even if this connection operates on a neurophysiological level.
The most commonly used method in this field of research is that of isolating the two partners, ensuring that there is no chance of sensorially obtaining information in the usual way, and the synchronous parallel recording of their respective neurophysiological activities. Therefore, one partner is stimulated at non-regular intervals with visual and auditory stimuli which can be structured, eg images, or non-structured, such as arrangements of black and white squares, or short duration sounds at a specific frequency. The choice to present the stimulations at irregular intervals, possibly also randomly, is important because it reduces neurophysiological autoactivation due to the expectation of stimulation.
At the end of the stimulation stage, each partner's recorded neurophysiological parameters are compared. If the non-stimulated partner's neurophysiological output shows activity that is simultaneous with activity in the stimulated partner, and this activity is statistically greater than during the non-stimulated periods, we can confirm that it derives from a mental connection, or at least from a means that is different from conventional electromagnetic transmission.

Regarding the type of correlation between the partners' neural activities, a further step with respect to simply proving its existence is determining whether it is aspecific or specific; this means whether the type of observed activity – for example in the activity of the partner receiving specific sensorial stimulations, such as a visual stimulation with an on-off modulation at 10 Hz and 14 Hz – is also seen in the mentally connected partner, or if the activation is undifferentiated, for example at 10 Hz.
As would be expected, in the correlated activities of the two partners, the neurophysiological activity of the non-stimulated partner is always smaller, and it could be that classical analysis methods are unable to separate the activity signal from the background.
Beginning in the last few years, thanks to the development of artificial intelligence algorithms, these machine-learning algorithms have been applied to the analysis of this neurophysiological activity (Chai et al., 2017; de Carvalho et al., 2017; Stober, Sternin, Owen, & Grahn, 2016; Lotte, Congedo, Lécuyer, Lamarche, & Arnaldi, 2007). Among their many advantages is the possibility of simultaneously analysing many variables that can be associated with a given event in both a linear and non-linear way, revealing coactivity configurations that would otherwise be difficult to see with other techniques. For an introduction to this type of algorithm see Lantz (2015).
Using these machine-learning techniques, this work re-analyzes data from two studies aiming to more precisely identify the neurophysiological parameters of the EEG activity of non-stimulated partners correlated to those produced by partners given specific sensorial stimulations.
The first group of data was obtained from a study by Giroldini et al., (2016). In this study, conducted using 25 pairs of participants, the stimulated partner was given a series of 128 continuous visual and auditory stimulations of 1 second duration at 500 Hz, separated by random intervals of

non-stimulation lasting from 4 to 6 seconds inclusive. Each partner's EEG activity was simultaneously recorded using 14-channel equipment.
The second group of data, product of an analysis conducted on 20 pairs of participants, is taken from a study by Giroldini, Pederzoli, Bilucaglia, Prati, & Tressoldi, (2018). In this study the stimulated partner was given random sequences of 32 visual stimulations of 1 second duration and an on-off modulation at 10, 12, or 14 Hz, while the EEG activities of each partner were simultaneously recorded.

Method.

First group of data

Participants
Six Italian Caucasian healthy adults were chosen for the experiment, comprised of five men and one woman, with an average age of 35.5 years (SD = 8.3).
They were selected from the members of EvanLab, the private laboratory involved in this study. The criteria for their voluntary inclusion were their mutual friendship (> 10 years), and their experience in being able to maintain prolonged focused concentration, a product of their familiarity with meditation and other practices requiring control of mental activities.
All together they contributed 25 different pairs.
The data were collected over three non-consecutive days. The dataset, available at http://dx.doi.org/10.6084/m9.figshare.1466876 including details of pairings, includes data from 14 EEG channels from 50 subjects (25 stimulated and 25 non-stimulated).

Procedure
Each stimulated subject received 128 audio-visual stimulations (AVS). The auditory stimulus was composed of a 500 Hz sinusoid applied through 32 Ohm Parrot ZIK® earphones at a volume of about 80 dB. The visual stimulation was from high intensity red LEDs in a 4×4 arrangement placed approximately one meter from the subject being stimulated. The subject kept his/her eyes closed because the light could easily be detected through the eyelids.
Additionally, for each subject (regardless of whether stimulated or not) 128 "surrogated" stimuli were drawn (nAVS). Their onsets were exactly 3 s before the AVS onsets in order to be differentiated from the nAVS by our classification algorithm.
All pre-processing steps were done in Matlab using the EEGLab toolbox (Delorme & Makeig, 2004).
After filtering with a zero-phase FIR band-pass filter $(2\sim40\mathrm{Hz})$, an ICA (Independent Component Analysis) was performed using a SOBI algorithm that, according to a previous study (Urigüen & Garcia-Zapirain, 2015), exhibits the best performance in the detection of the artefacts.
ICs (Independent Components) corresponding to artefacts were automatically identified and rejected using the MARA algorithm (Winkler, Haufe, & Tangermann, 2011) that is based on a set of spatial, temporal and statistical features. Finally, a CAR (Common Average Reference) was performed.
Given that this type of stimulation produced a P300-like wave, we followed the common procedures used with Brain Computer Interfaces based on P300 (e.g. Hoffmann, Vesin, Ebrahimi, & Diserens, 2008). Data were first epoched $1\ \mathrm{s}$ after the stimulus onset, then a sixth order Butterworth bandpass filter $(1\sim12\ \mathrm{Hz})$ was applied and downsampled to $32\ \mathrm{Hz}$. Epoch lengths were thus lowered to 64 samples located at time points:

$$\{t_k\}_{k=1}^{64} = \{0s,\ -0.6667s, \ldots, +1.2333s, +1.2667s\}.$$

Samples were then amplitude-scaled according to the maximum and the minimum value inside each epoch, according to the equation:

$$x_{scaled} = \frac{x - \frac{(x_{max} + x_{min})}{2}}{\frac{(x_{max} - x_{min})}{2}}$$

Finally, scaled samples were concatenated to form a feature vector v, with a dimensionality of $65 \times 14 = 910$:

$$v = [x_1(t_1), x_1(t_2), \dots, x_1(t_{64}), \dots x_k(t_j), \dots x_{14}(t_1), x_{14}(t_2), \dots x_{14}(t_{64})]$$

where $x_k(t_j)$ is the sample at time point t_j from channel k.

Feature selection

Reduction of the feature dimensionality is crucial to improve classification performances. A simple method for feature selection is based on the ranking of the Biserial Correlation Coefficients (Müller, Krauledat, Dornhege, Curio, & Blankertz, 2004). Considering a two-class dataset D (with just one numerical feature), the Biserial Correlation Coefficient r^2 for the feature is defined as:

$$r^2 = \left(\frac{\sqrt{N_A \cdot N_B}}{N_A + N_B} \frac{m(D_A) - m(D_B)}{s(D)} \right)$$

where D_A, D_B are the subsets of the dataset D composed by instances that belong to class A, B. $m(\cdot)$ and $s(\cdot)$ are, respectively, the sample mean and standard deviation operators. r^2 score is a measure of the "discriminative power" of the feature, reflecting how much of its "variance" is "explained" by the class affiliation.

After adding the coefficients of each feature and sorting the scores in descending order, we selected the features of which the added score came to 95% of the total score.

For each stimulated and non-stimulated group of participants, the scalp distributions of r^2 coefficients (expressed as percentage, normalized to the total score) were drawn. Since each channel is associated with at most 65 features (as well as 65 r^2 coefficients), coefficients (1 coefficient for each channel) are calculated as mean value.

Classification

As classifier, we chose a Linear Discriminant (LD) classifier and the estimation of the classification accuracy was performed 10 times (to compensate for the random variability of the estimated accuracy) by a 10-fold stratified cross-validation scheme.

We choose LD because, according to the literature (Lotte, Congedo, Lécuyer, Lamarche, & Arnaldi, 2007) it has a very low computational requirement, is simple to use and generally provides good results (i.e. robustness to overfitting).

Since the feature selection is performed using information from the class labels, in order to avoid overfitting and to train the classifier in a "fair way", feature selection was performed at each step within the cross-validation.

In addition to the LD classifier, at each step we classified our data using a Random classifier (which gets a prediction uniformly distributed between the classes) that serves as a "baseline" to evaluate the LD classifier performance. The random classification is simply obtained randomly assigning (with uniform probability p=1/n) to each instance of the test set one of the class {C_1,C_2,…,C_n}, where n is the number of classes to be predicted.

At each cross-validation step, we calculated the mean accuracy and, finally, we calculated the mean and standard deviation of these mean accuracies.
The syntax in MatLab code is available here: https://figshare.com/s/865345260fbe637b0a73

Results

Figure 1 and Figure 2 show the scalp distributions of r^2 coefficients (expressed as percentage, normalized to the total score) for the stimulated and non-stimulated participants, respectively.
As shown in Figure 1, the class-discrimination (AVS vs nAVS) in the stimulated participants derives mostly from central and left frontal and right temporal electrodes, while in the non-stimulated participants their class is best distinguished by features from the right temporal and left occipital electrodes.

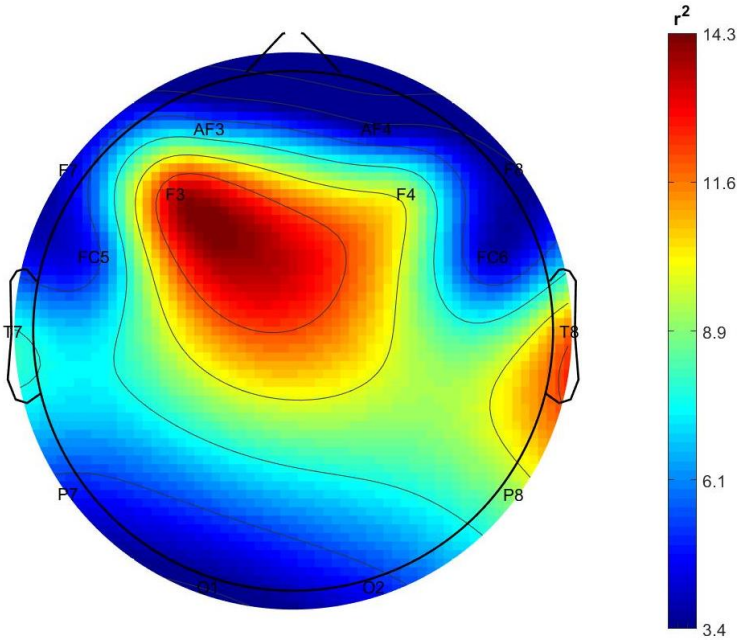

Figure 1 - Topographic distribution of r^2 coefficients in the stimulated participants.

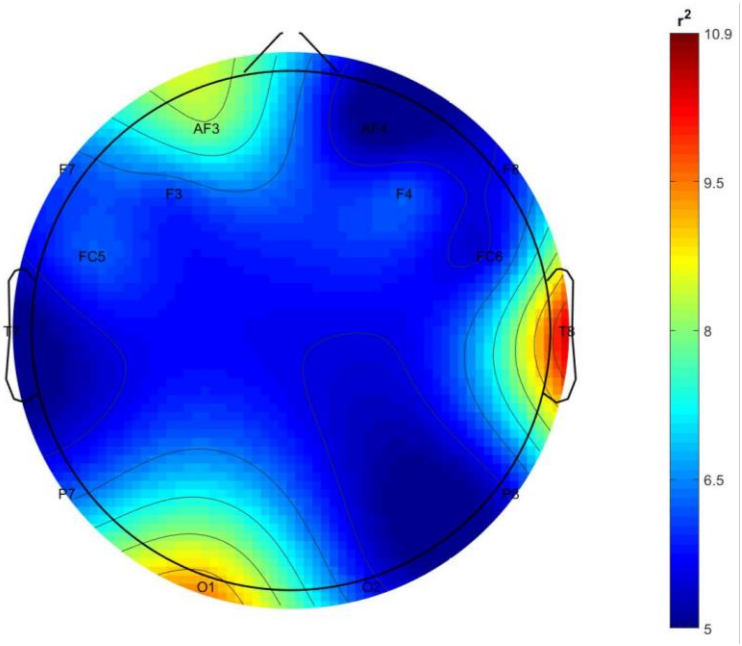

Figure 2: Topographic distribution of r^2 coefficients in the non-stimulated participants.

The percentages of the classification accuracy are reported in Table 1 and Table 2 for the stimulated and the non-stimulated participants, respectively.

Table 1: Percentages of the classifications for the stimulated participants. LDA: linear discriminant analysis; Random: random classifier.

	LD	**Random**
Iteration #1	82.76	49.84
Iteration #2	82.95	50.58
Iteration #3	82.98	49.33
Iteration #4	82.78	49.64
Iteration #5	82.72	51.42
Iteration #6	82.58	49.91
Iteration #7	83.09	50.62
Iteration #8	82.86	51.10
Iteration #9	82.68	50.30
Iteration #10	83.00	50.34
Mean	82.84	50.31
SD	0.16	0.65

Table 2: Results of the classifications for the non-stimulated participants

	LD	**Random**
Iteration #1	51.32	49.33
Iteration #2	51.09	49.81
Iteration #3	49.81	49.78
Iteration #4	51.06	48.96
Iteration #5	51.09	50.16
Iteration #6	50.33	50.95
Iteration #7	50.42	50.64
Iteration #8	50.95	49.72
Iteration #9	50.97	51.29
Iteration #10	50.34	50.30
Mean	50.74	50.09
SD	0.48	0.72

Inferential statistics and parameters estimation

For the inferential statistics we chose the comparison of percentage of correct discrimination between the stimulation and non-stimulation conditions, comparing each with the percentage obtained with the Random Classifier using a one-tailed paired t-test and a comparison using the Bayes Factor calculation using the default Cauchy prior value. As a parameter estimation, we chose

the measurement of Cohen's effect size *d* and the relative confidence interval of 95%, all one-directional. All statistical analyses were conducted using Jasp software (Jasp Team, 2018). Results are presented in Table 3 below, while data from the Bayes Factor Robustness Check are shown in the Supplementary Material.

Table 3: Inferential statistics and parameters estimation of the comparison between the percentage of correct classification between the linear discriminant and the random classifiers.

	Stimulated participants	**Non-stimulated participants**
t-test (*p*-value)	154.84 (<.001)	2.06 (.035)
Cohen's *d* (lower 95% CI)	48.9 (28.6)	.65 (.06)
Bayes Factor $_{H1/H0}$	2.32^{e13}	2.63

Comment
While results for the stimulated participants were as expected, those observed from non-stimulated participants were interesting. Indeed, even if the correct discrimination percentage is not particularly high, all the inferential statistics and parameter estimates indicate the presence of an EEG signal corresponding to stimulation periods. Furthermore, the origins of these differences (see Figure 2) correspond to channels T8 and O1, which correspond to brain areas involved in processing auditory and visual information respectively.

Second group of data

The dataset is composed of 14-channel EEG data obtained from 20 pairs of participants and is available here: http://tidy.ws/bpiaKe.

Participants
Five adults, two women and three men with an average age of 38.3 years (SD = 7.5), took part in this study. The selection criteria were their experience in mind control techniques (mainly meditation) and their mutual friendship, which we consider as essential pre-requisites for an adequate "mental and emotional connection" between the pairs. Each participant took turns in being both the stimulated partner and the non-stimulated partner with each of the others, making a total of 20 pair combinations.
This sample size of 20 pairs of participants was estimated by setting the following parameters: statistical power = .80, a one-tailed Type I error = .05 and an expected effect size *d* = .5 for a one sample t-test (difference from a constant = 0: http://powerandsamplesize.com/Calculators/Test-l - Mean/1-Sample-1-Sided).

Stimuli
Visual stimuli consisted of red light flashes at 10, 12, 14 Hz (32 stimuli for each frequency) lasting 1 s with a minimum inter-stimulus interval of 4 s, while audio stimuli consisted of a 900 Hz sine tone, modulated on-off at the flashing frequencies.
The audio modulation was performed on a 900 Hz sinusoidal carrier and applied through 32 ohm impedance earphones at a volume of about 80 dB.
The interval between the three blocks was randomly varied at between 40 and 90 seconds.
The visual stimuli were provided by an array of 16 red LEDs positioned about 30 cm from the stimulated partner's closed eyes.
The three frequency blocks were presented randomly without repetition of the same frequency.

Additionally, for each subject (regardless of whether stimulated or not) the onsets of 32 "surrogated" stimuli (0 Hz) were drawn from random positions of the entire recording: the first and the last 10 s were discarded, maintaining the same minimum inter-stimulus distance.

Preprocessing

All pre-processing steps were done as for the first dataset. Data were epoched with a 2s window after each stimulus onset. From each epoch and each channel the PSD (Power Spectral Density) was estimated with a Welch's periodogram (1 s long Hamming window with 50% of overlap) and spectral bins were normalized to the maximum value of the PSD.
Following the feature extraction procedure normally used with Brain-Computer-Interfaces systems based on SSVEP (e.g. Müller-Putz, Scherer, Brauneis, & Pfurtscheller, 2005), we concatenated spectral bins corresponding to both stimulus frequencies and their first harmonics:
$F = \{10, 20;\ 12, 24;\ 14, 28\}$ Hz.
The feature vector v, with a dimensionality of $6 \times 14 = 84$, is thus defined as:

$$v = [p_1(10), p_1(20), \dots, p_k(f_j), \dots, p_{14}(14), p_{14}(28)\ ]$$

where $p_k(f)$ is the spectral power at frequency $f_j \in F$ from channel k.

Feature selection

The 4-class (10, 12, 14, 0) prediction problem was decomposed into 6 different 2-class prediction problems, creating 6 different datasets containing all possible pairings of the 4 classes: $\{10, 12\}$, $\{10,14\}$, $\{10,0\}$, $\{12, 14\}$, $\{12,0\}$ and $\{14, 0\}$.
Feature selection was based on the ranking of the Biserial Correlation Coefficients as with the first dataset.

Classification

As classifier, we used a Linear Discriminant (LD) classifier compared to a Random classifier, as with the first dataset. Again, we performed a 10-fold stratified cross-validation scheme, with feature selection inside each cross-validation step.

Results

Figure 3 and 4 show the scalp distributions of the mean r^2 coefficients (expressed as percentage, normalized to the total score) for each 2-class problem for each group (stimulated and non-stimulated pairs).

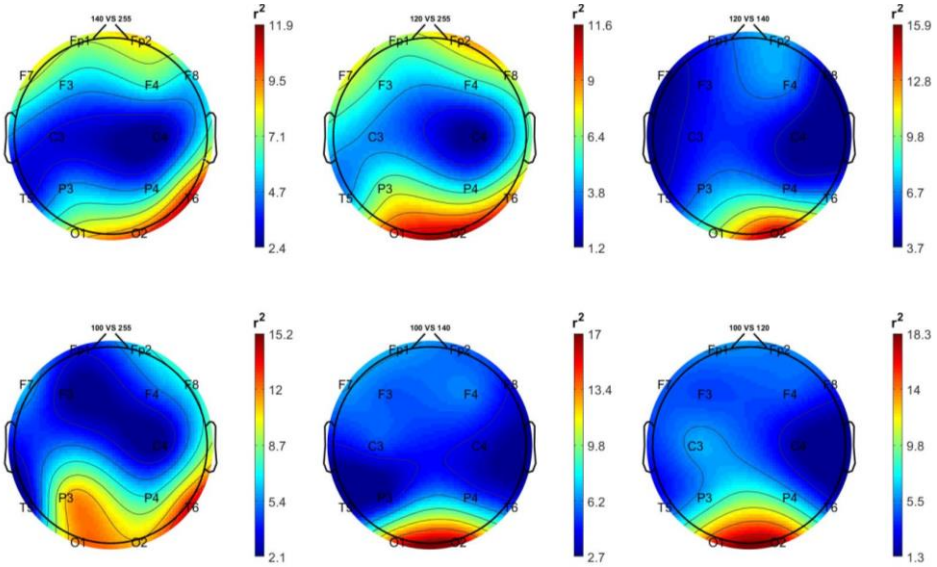

Figure 3: Topographic distribution of r^2 coefficients of the stimulated participants. Top left: 14 Hz vs 0 Hz; top centre: 12 Hz vs 0 Hz; top right: 12 Hz vs 14 Hz; bottom left: 10 Hz vs 0 Hz; bottom centre: 10 Hz vs 14 Hz; bottom right; 10 Hz vs 12 Hz.

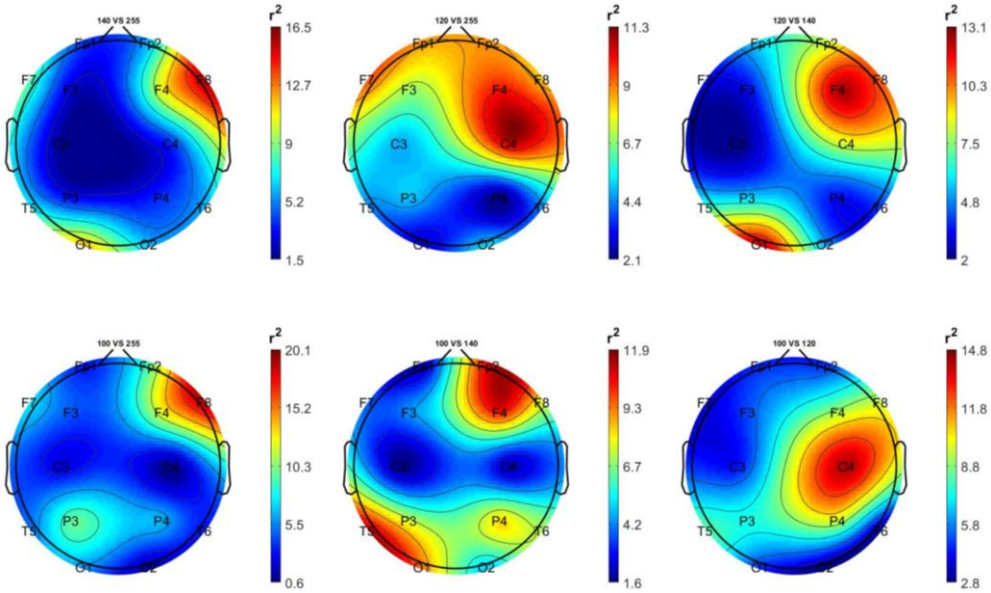

Figure 4: Topographic distribution of r^2 coefficients of the non-stimulated participants. Top left: 14 Hz vs 0 Hz; top centre: 12 Hz vs 0 Hz; top right: 12 Hz vs 14 Hz; bottom left: 10 Hz vs 0 Hz; bottom centre: 10 Hz vs 14 Hz; bottom right; 10 Hz vs 12 Hz.

Comment

As shown in Figure , in the stimulated participants the EEG activity generated by the three frequencies of stimulation is best distinguished from the 0 Hz class (non-stimulation) by the right occipital and temporal regions' features.

In the non-stimulated participants (Figure 4), the 10 Hz and 14 Hz are best distinguished from the 0 Hz class by frontal and frontocentral regions features.

Percentages of classification accuracy

The percentages of correct classification for each comparison for each of the 10 cross-validation iterations and their descriptive statistics observed in the stimulated participants are visible in Table 4.

Table 4: Percentages of classification accuracies for the stimulated participants

	10Hz vs 0Hz		12Hz vs 0Hz		14Hz vs 0Hz	
	LD	**Random**	**LD**	**Random**	**LD**	**Random**
Iteration #1	70.39	50.47	71.95	50.70	72.27	50.23
Iteration #2	71.25	49.30	72.50	47.66	72.42	49.38
Iteration #3	70.55	50.00	71.64	50.39	72.27	50.63
Iteration #4	69.84	49.45	73.05	51.56	71.72	50.31
Iteration #5	69.22	51.41	72.73	51.33	71.48	48.36
Iteration #6	69.84	50.31	73.05	51.88	71.72	50.94
Iteration #7	70.70	50.00	72.34	48.52	72.19	53.05
Iteration #8	70.08	48.91	72.03	48.83	72.11	50.63
Iteration #9	69.61	49.69	72.34	50.55	72.58	50.23
Iteration#10	69.61	50.16	72.19	51.41	72.11	52.42
Mean	**70.11**	49.97	**72.38**	50.28	**72.09**	50.62
SD	0.61	0.69	0.46	1.38	0.34	1.34

Inferential statistics and parameters estimation

Similarly to the first dataset, for the inferential statistics we chose the comparison with the percentage of correct discrimination between the three stimulation conditions at 10 Hz, 12 Hz, and 14 Hz, and the non-stimulation (0 Hz), comparing each with the percentages obtained from the Random Classifier using a paired one-tailed t-test and a comparison by way of the Bayes Factor calculation using the default Cauchy prior value. As a parameter estimate, we chose Cohen's *d* and the relative confidence interval of 95%, all one-directional. These results are presented in Table 5, while the Bayes Factor Robustness Check data are shown in the Supplementary Material.

Table 5: Results of paired-t test, Bayes Factor ($BF_{H1/H0}$) and Cohen's *d* of the comparison between the different variables in the stimulated participants.

LD	**Random**	**t-test**	***p***	***d***	**95%CI-Inf**	**BF_{10}**
10 Hz vs 0	10 Hz vs 0 r	56.95	< .001	18.01	10.92	7.45e ^{9}
12 Hz vs 0	12 Hz vs 0 r	51.32	< .001	16.23	9.84	3.26e^{9}
14 Hz vs 0	14 Hz vs 0 r	51.91	< .001	16.42	9.95	3.57e^{9}

Comment

As seen from the averages, the percentage of correct classification of EEG activity between the non-stimulation and stimulation periods with the three frequency values is always greater than 70%, as confirmed by the inferential statistics results.

The percentages of correct classification of each comparison for each of the 10 cross-validation iteractions and their descriptive statistics observed in the non-stimulated participants are presented in Table 6.

Table 6: Percentages of classification accuracies for the non-stimulated participants

	10Hz vs 0Hz		12Hz vs 0Hz		14Hz vs 0Hz	
	LD	**Random**	**LD**	**Random**	**LD**	**Random**
Iteration #1	51.33	49.45	52.19	47.66	52.11	50.94
Iteration #2	50.78	50.47	50.16	48.83	51.64	50.31
Iteration #3	51.41	49.53	50.16	51.09	52.73	48.91
Iteration #4	52.27	48.67	51.56	49.84	53.44	48.75
Iteration #5	52.97	49.45	50.39	52.19	50.78	46.80
Iteration #6	50.47	50.39	49.69	47.58	50.16	51.09
Iteration #7	50.39	49.77	50.55	49.30	51.56	47.97
Iteration #8	52.42	52.50	48.52	50.08	52.42	49.14
Iteration #9	50.63	49.84	50.08	51.33	53.52	50.47
Iteration#10	49.06	50.47	51.25	51.09	50.78	48.28
Mean	**51.17**	50.05	**50.45**	49.90	**51.91**	49.27
SD	1.15	1.02	1.02	1.56	1.14	1.4

Inferential statistics and parameters estimation

Results of inferential statistics and parameter estimates are shown in Table 7.

Table 7: Results of paired-t test, Bayes Factor ($BF_{H1/H0}$) and Cohen's d of the comparison of the different variables in the non-stimulated participants.

LD	**Random**	**t-test**	***p***	***d***	**95%CI-Inf**	**$BF_{H1/H0}$**
10 Hz vs 0	10 Hz vs 0r	2.21	0.027	0.70	0.09	3.19
12 Hz vs 0	12 Hz vs 0r	0.87	0.202	0.27	-0.26	0.66
14 Hz vs 0	14 Hz vs 0r	4.97	< .001	1.57	0.75	101.98

Comment

The most interesting result is that at least two out of the three stimulation frequencies, 10 Hz and 14 Hz, are classified as greater than chance with respect to the non-stimulation condition, even if more obvious at 14 Hz.

Discussion

The machine-learning re-analyses of data from two studies relative to the distant correlation between EEG activity of participant pairs who were sensorially stimulated and participants who were connected only mentally not only confirmed the existence of a correlation, as shown in the two studies from which they were taken, but also pointed out the degree of classification between stimulated and non-stimulated conditions depended on the stimulation frequency used.

Even though, with hindsight, the choice to use frequencies that are compatible with or close to the Alpha state was not optimal, seeing as the dominant EEG activity in non-stimulated participants was compatible with this EEG state, the evidence that these are distinguishable even in the EEG activity of non-stimulated participants opens interesting possibilities, should this research path be continued in terms of practical applications.

From a theoretical point of view, while we can safely reject the theory that the observed activity in non-stimulated participants is due to a traditional sensorial transmission (albeit weak) of stimulated participants' EEG activity, we as yet do not have enough information to determine if this correlation – which does not necessarily involve transmission – has the same characteristics as that seen in quantum mechanics. Indeed, to determine this it would, first of all, entail closing a series of loopholes, as was done in quantum mechanics to reject the theory that distant connection used the laws of classical physics (Giustina et al., 2015; Shalm et al., 2015). For example, the loophole showing the impossibility of communication at the speed of light between participant pairs would need closing.

Pending a better understanding of the laws regulating the correlation between the EEG activity of two mentally-connected participants, we believe however that data obtained so far in this field, including that of other researchers, clearly show that if classification algorithms of signals down to the level of single participants are perfected, the road towards practical use of mental telecommunication can be opened, even if for now it is based on binary or more complex symbolic codes.

Mental telecommunication, not just those based on electromagnetic waves but also those of the future based on quantum technologies, have the advantage of not requiring repeaters or security measures and would certainly be beneficial from an economical point of view.

References

Chai, R., Ling, S. H., San, P. P., Naik, G. R., Nguyen, T. N., Tran, Y., … Nguyen, H. T. (2017). Improving EEG-Based Driver Fatigue Classification Using Sparse-Deep Belief Networks. *Frontiers in Neuroscience*, *11*, 103. https://doi.org/10.3389/fnins.2017.00103

de Carvalho, S. R., Filho, I. C., de Resende, D. C. O., Siravenha, A. C. Q., Meiguins, B. S., Debarba, H. G., & Gomes, B. D. (2017). A Novel Procedure for Classification of Early Human Actions from EEG Signals. In *2017 Brazilian Conference on Intelligent Systems (BRACIS)* (pp. 240–245). IEEE. https://doi.org/10.1109/BRACIS.2017.39

Galli Carminati, G., Martin, F., & Carminati, F. (2017). A Very Simple Quantum Model of Mind and Matter. *NeuroQuantology*, *15*(2). https://doi.org/10.14704/nq.2017.15.2.1031

Giroldini, W., Pederzoli, L., Bilucaglia, M., Caini, P., Ferrini, A., Melloni, S., … Tressoldi, P. (2016). EEG correlates of social interaction at distance. *F1000Research*, *4*, 457. https://doi.org/10.12688/f1000research.6755.5

Giroldini, W., Pederzoli, L., Bilucaglia, M., Prati, E., & Tressoldi, P. (2018). Exploring the Brain-to-Brain interaction at a distance: a global or differential relationship? https://doi.org/10.31234/OSF.IO/Z8D65

Giustina, M., Versteegh, M. A. M., Wengerowsky, S., Handsteiner, J., Hochrainer, A., Phelan, K., … Zeilinger, A. (2015). Significant-Loophole-Free Test of Bell's Theorem with Entangled Photons. *Physical Review Letters*, *115*(25), 250401. https://doi.org/10.1103/PhysRevLett.115.250401

Hoffmann, U., Vesin, J.-M., Ebrahimi, T., & Diserens, K. (2008). An efficient P300-based brain–computer interface for disabled subjects. *Journal of Neuroscience Methods*, *167*(1), 115–125. https://doi.org/10.1016/J.JNEUMETH.2007.03.005

Jiang, L., Stocco, A., Losey, D. M., Abernethy, J. A., Prat, C. S., & Rao, R. P. N. (2018). BrainNet: A Multi-Person Brain-to-Brain Interface for Direct Collaboration Between Brains. *ArXiv*.

Lantz, B. (2015). *Machine learning with R : discover how to build machine learning algorithms, prepare data, and dig deep into data prediction techniques with R*. Packt Publishing.

Lee, W., Kim, S., Kim, B., Lee, C., Chung, Y. A., Kim, L., & Yoo, S.-S. (2017). Non-invasive transmission of sensorimotor information in humans using an EEG/focused ultrasound brain-to-brain interface. *PLOS ONE*, *12*(6), e0178476. https://doi.org/10.1371/journal.pone.0178476

Lotte, F., Congedo, M., Lécuyer, A., Lamarche, F., & Arnaldi, B. (2007). A review of classification algorithms for EEG-based brain–computer interfaces. *Journal of Neural Engineering*, *4*(2), R1–R13. https://doi.org/10.1088/1741-2560/4/2/R01

Müller-Putz, G. R., Scherer, R., Brauneis, C., & Pfurtscheller, G. (2005). Steady-state visual evoked potential (SSVEP)-based communication: impact of harmonic frequency components. *Journal of Neural Engineering*, *2*(4), 123–130. https://doi.org/10.1088/1741-2560/2/4/008

Müller, K., Krauledat, M., Dornhege, G., Curio, G., & Blankertz, B. (2004). Machine learning techniques for brain-computer interfaces. *Biomedizinische Technik*, *49*(1), 11–22.

Shalm, L. K., Meyer-Scott, E., Christensen, B. G., Bierhorst, P., Wayne, M. A., Stevens, M. J., … Nam, S. W. (2015). Strong Loophole-Free Test of Local Realism. *Physical Review Letters*, *115*(25), 250402. https://doi.org/10.1103/PhysRevLett.115.250402

Stober, S., Sternin, A., Owen, A. M., & Grahn, J. A. (2016). Deep Feature Learning for EEG Recordings. *ArXiv*.

Urigüen, J. A., & Garcia-Zapirain, B. (2015). EEG artifact removal—state-of-the-art and guidelines. *Journal of Neural Engineering*, *12*(3), 031001. https://doi.org/10.1088/1741-2560/12/3/031001

Walach, H., & Römer, H. (2011). Generalized Entanglement - A Nonreductive Option for a Phenomenologically Dualist and Ontologically Monist View of Consciousness. In *Studies in Neuroscience, Consciousness and Spirituality l* , (pp. 81–95). Berlin, Heidelberg: Springer Science Business Media. https://doi.org/10.1007/978-94-007-2079-4_6

Walach, H., Tressoldi, P., & Pederzoli, L. (2016). Mental, behavioural and physiological nonlocal correlations within the Generalized Quantum Theory framework. *Axiomathes*, *26*(3), 313–328. https://doi.org/10.1007/s10516-016-9290-6

Winkler, I., Haufe, S., & Tangermann, M. (2011). Automatic Classification of Artifactual ICA-Components for Artifact Removal in EEG Signals. *Behavioral and Brain Functions*, *7*(1), 30. https://doi.org/10.1186/1744-9081-7-30

SUPPLEMENTARY MATERIAL

Dataset 1
Stimulated participants: Bayes Factor Robustness Check

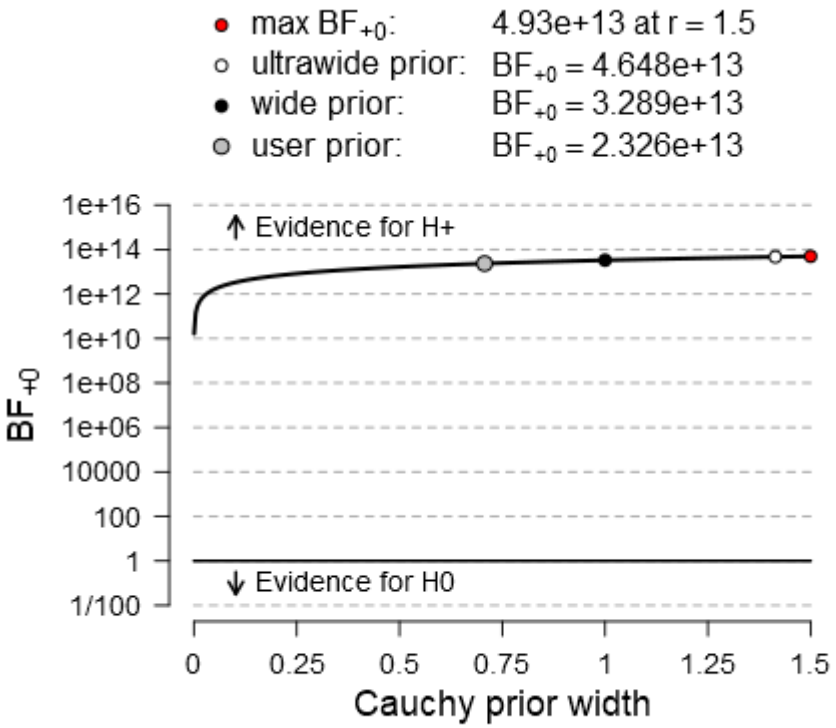

Non-stimulated participants: Bayes Factor Robustness Check

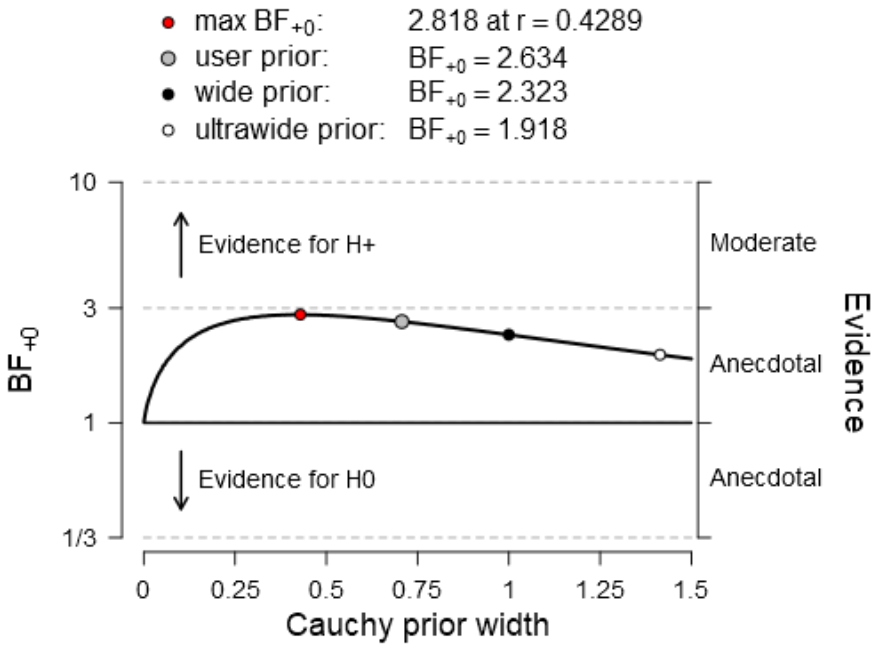

Dataset 2
Non-stimulated participants
Bayes Factor Robustness Check: **10 Hz vs 0 Hz**

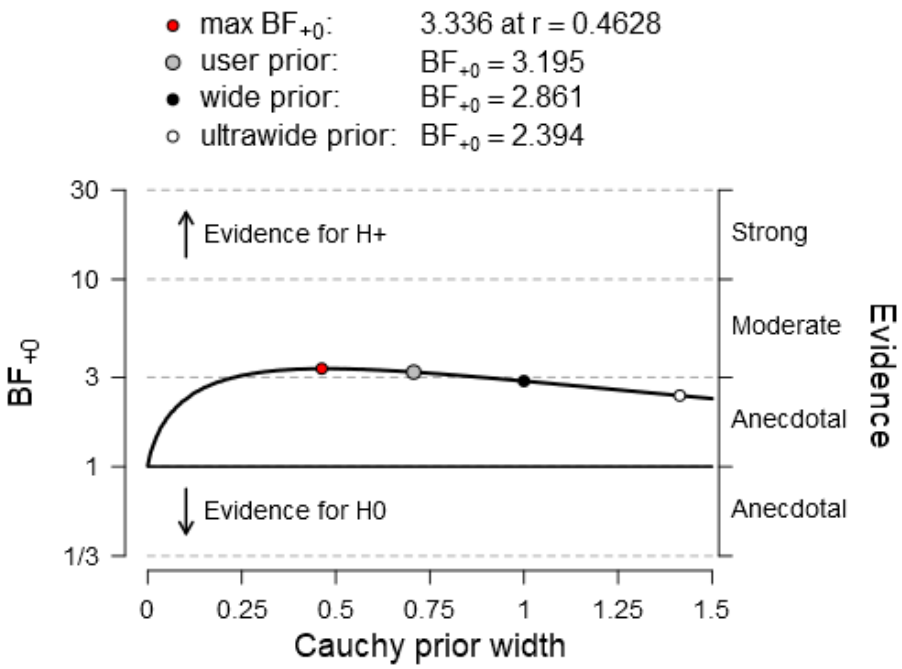

Bayes Factor Robustness Check: **14 Hz vs 0 Hz**